

Interstellar Scintillation of PSR J0437–4715 on Two Scales [★]

C.R. Gwinn¹, C. Hirano¹, and S. Boldyrev²

¹ Department of Physics, University of California, Santa Barbara, CA 93106, USA e-mail: cgwinn@physics.ucsb.edu

² Department of Astronomy and Astrophysics, University of Chicago, Chicago, IL 60637, USA e-mail: boldyrev@flash.uchicago.edu

Received 00.00.05 / Accepted 00.00.05

ABSTRACT

Aims. We sought to determine the scale of scintillation in the interstellar plasma of PSR J0437–4715.

Methods. We used the US VLB Array to obtain scintillation amplitude and phase data, from dynamic spectra at 327 MHz.

Results. We observe two scales of scintillation of pulsar PSR J0437–4715, differing by more than an order of magnitude in scintillation bandwidth. The wider-bandwidth scale of scintillation that we observe indicates less scattering for this pulsar than for other nearby pulsars, other than PSR B0950+08. The narrower scale agrees approximately with that observed for other nearby pulsars.

Key words. turbulence – pulsars: individual (PSR J0437–4715)

1. Introduction

In this paper we report measurement of the interstellar scattering by plasma along the line of sight to pulsar J0437–4715. This is one of the closest pulsars. It has distance $R = 150$ pc, and its transverse velocity is 100 km/sec (van Straten 2001). It is quite strong over a wide range of observing frequencies. Its proximity, and its intensity, make it an important probe of the local interstellar plasma.

We describe observations of the scattering parameters of J0437–4715, made at 327 MHz. We find two scales of scintillation, corresponding to two scales of structure in the pulsar’s dynamic spectrum. Multiple scales are not uncommon for nearby pulsars (see, for example, Stinebring et al. 2001, Hill et al. 2003), although scales separated by an order of magnitude are unusual. Comparison with other pulsars of similar distance and dispersion measure shows that this pulsar has relatively less scattering than expected on the basis of a model for homogeneous turbulence. In this paper, we discuss the observations and comparison with other pulsars. We discuss comparison with previous observations of scintillation of J0437–4715, and interpretation of the measurements, in an accompanying paper (Smirnova et al. 2005), hereafter Paper 2).

2. Observations and Analysis

2.1. Data Collection and Calibration

We observed PSR J0437–4715 at two epochs using the Very Long Baseline Array (VLBA) operated by the National Radio Astronomy Observatory (NRAO). On 5 November 1996, we observed the pulsar over four 33-minute scans, using 25-meter telescopes at Fort Davis, Mauna Kea, Pie Town, and St. Croix, with a 32-MHz bandwidth centered at 332 MHz, and with a 250-kHz spectral resolution. Between the scans, we observed extragalactic sources for calibration purposes. On 8 April 1999, we observed the target for two 44-minute scans and one 33-minute scan, using the telescopes at Fort Davis, Kitt Peak, Los Alamos, Mauna Kea, Owens Valley, Pie Town, and St. Croix, with a bandwidth of 32 MHz centered at 328 MHz, and with a spectral resolution of 125 kHz. Mutual visibility is short, particularly on long baselines, because the source lies at low declination; this limited the useful time span of the observations. To increase the signal-to-noise ratio, the data for this observation were correlated using a gate which covered 12% of the pulse period and which isolated the central peak of the pulse profile. Scans of a calibrator source preceded and succeeded the observations of the pulsar. For both observations, we aggregated the 32-MHz bandwidth using four 8-MHz intermediate-frequency (IF) bands.

We performed the first half of the calibration using NRAO’s Astronomical Image Processing System (AIPS). The data from both observations were marred by radio-frequency interference (RFI). The second observation in particular suffered badly from RFI, forcing us to eliminate the Kitt Peak and Owens Valley antennas from the outset. The interference also tainted some

[★] Observations made with the US VLBA. The National Radio Astronomy Observatory is a facility of the National Science Foundation operated under cooperative agreement by Associated Universities, Inc.

measurements of system temperature. The system temperature should not change abruptly, so if an isolated reading clearly departed from an otherwise smooth trend, we removed that value. In two IFs, however, rampant corruption due to RFI obliterated evidence of a smooth evolution in system temperature. For these two IFs, we copied the system temperatures from an adjacent IF.

We examined the remaining visibilities and flagged channels and time ranges to eliminate data corrupted by very strong, narrow-band signals typical of man-made sources. We applied the usual corrections for the effects of antenna parallactic angles, digital sampler bias, system temperature, and gain calibration. We then performed a manual phase calibration by running a fringe fit on a thirty-second interval of calibrator data to determine the electronic delay differences between IFs, and we removed the resulting phase differences from the pulsar and calibrator data. The final procedure done using AIPS was a fringe fit on each source to remove phase slopes due to the residual fringe rate and delay.

To perform a bandpass calibration, we averaged, for each baseline, the complex visibilities from a ten-minute interval of calibrator data. Deviations from a flat amplitude and phase spectrum reflected the non-ideal frequency response of the baseband converters. The gain of the filters drops off at the ends of each IF, significantly reducing the signal-to-noise ratio in the first and last channel of each IF; consequently, we omitted these channels in our subsequent analysis. We then smoothed the data using boxcar averaging with a one-minute window to further increase the signal-to-noise ratio. We then exported the data from AIPS and continued calibration using custom software.

At our observing frequency, propagation through the ionosphere significantly affects the visibility phases (Thompson et al. 1986). Data from both observations exhibited broadband variations in phase of order half a radian over a time scale of about fifteen minutes, as would be expected for ionosphere path changes. We approximated and removed these variations using an eighth-order polynomial fit to amplitude-weighted phase averages calculated for each time point.

The ionosphere also induced phase curvature in frequency. The fringe fit removes the first-order dependence of phase on frequency, and usually, the bandwidth is small enough compared to the observing frequency that the second-order term is not important. However, in our case, the bandwidth was approximately 10% of the observing frequency, and the resulting 1% second-order correction could be of order a radian for typical values of total electron content for the ionosphere. We fit the amplitude-weighted phase averages calculated for each channel to a quadratic polynomial and used this polynomial to calculate the appropriate phase to subtract from the visibilities in each channel. This yielded the amplitude as a function of frequency, as shown for example in Figure 1 for the short Fort Davis-Pie Town baseline.

To verify that our calibration procedure did not introduce any unintended biases, we calculated two-dimensional autocorrelation functions (ACF) for each data set using the visibilities from a calibrator source. As expected, we obtained results flat in both time and frequency lags, except for a spike at small time

and frequency lags due to the effects of noise, broadened from a delta-function by smoothing.

2.2. Observational Results

2.2.1. Dynamic Spectra

Initially, we had hoped to measure the angular broadening of the pulsar by measuring the phase variations of the diffraction pattern; however, several complications derailed our efforts. Most significantly, the scintillation bandwidth was much larger than expected. As the phase variations of the diffraction pattern have this characteristic bandwidth (Desai et al. 1992), they could not be distinguished from ionospheric phase, phase slope, and curvature. Moreover, the angular scale inferred from the scintillation bandwidth is so small that we would not expect to detect phase variations on any Earth-based baseline, at 327 MHz or higher observing frequency.

We chose to focus on the Fort Davis-Pie Town baseline, which had the least interference and best signal-to-noise ratio. Figure 1 shows plots of the visibility amplitudes for the pulsar on this baseline for both epochs. The white vertical lines correspond to the channels omitted at the ends of each IF, and the white horizontal lines correspond to breaks in the scan or to time ranges flagged because of RFI. At both epochs, we detected scintillation maxima that typically persist for ten to twenty minutes and that span several IFs, suggesting a characteristic width in frequency on the order of ten megahertz.

2.2.2. Scintillation Bandwidth and Timescale

We formed autocorrelation functions of the data shown in Figure 1. Figure 2 shows an example, a composite autocorrelation function formed for all the data. We then fit models to the autocorrelation functions, using the form expected for Gaussian spectra: a Lorentzian for differences in frequency and a Gaussian for differences in time (see Gwinn et al. 1998). We found values of $\Delta\nu = 14.7 \pm 0.5$ MHz for the first epoch and $\Delta\nu = 16.5 \pm 0.5$ MHz for the second, measured as the half-width at half maximum of the autocorrelation function. The quoted errors are standard errors for the fit; we discuss the expected uncertainties further below. The measured scintillation timescales were $t_{ISS} = 885 \pm 9$ s for the first epoch and $t_{ISS} = 1630 \pm 80$ s for the second, measured as the time at which the Gaussian component of the correlation function declines to $1/e$ of its peak value.

As Figure 1 shows, the number of independent samples with these dimensions is small, so that the accuracy of our measurement is limited by number of samples. Phillips & Clegg (1992) argue that the fractional accuracy of such a measurement is given by the number of independent samples, so that

$$\sigma(\Delta\nu)^2/\Delta\nu = 1/(N_t \times N_f) = t_{ISS}/T \times \Delta\nu/B. \quad (1)$$

For our observations, $T/t_{ISS} \approx 14$, and $B/\Delta\nu \approx 2$. We thus expect $\sigma(\Delta\nu) \approx (1/\sqrt{28})\Delta\nu \approx 3$ MHz.

Because the total bandwidth is only twice the decorrelation bandwidth, we used Monte Carlo simulations with a range

of parameters to estimate errors as well. Using the stationary-phase technique (Gwinn et al. 1998), we formed 1500 dynamic spectra with the same N_i and N_f as our observations, with “true” decorrelation bandwidth evenly distributed between 0 and 50 MHz. We then found the autocorrelation function for these synthetic spectra, and fitted for the decorrelation bandwidth, as described above for the actual data. We then found the distribution of “true” decorrelation bandwidth that contributed to Monte Carlo results close to our measured value. Thus, we inferred a parent distribution for our observed value.

We found that the parent distribution was sharply peaked near the measured value of 16 MHz, but had an extended tail toward larger values. Of those spectra that yielded values near our measured value, 67% came from the interval between 13 MHz and 24 MHz. The endpoints of this interval have about equal probability, according to our Monte Carlo simulations; their asymmetry about the most probable value of 16 MHz reflects the tail toward larger $\Delta\nu$. The fact that we obtain values close to 16 MHz independently, from both of our observing epochs, provides additional evidence that 16 MHz is the “true” underlying value; we did not demand that our Monte Carlo simulations reproduce this additional fact, to keep them manageable simple. This simulation suggests that the uncertainty suggested by Eq. 1 is approximately correct, with additional probability on the side toward larger $\Delta\nu$.

The Monte Carlo simulations indicate that the actual decorrelation bandwidth is unlikely to be about 1 MHz, as would be expected from some previous measurements (see 2005). To test this hypothesis, we formed 1000 spectra with true decorrelation bandwidth of 1 MHz, and then found the autocorrelation function and fitted value for the decorrelation bandwidth. None approached 16 MHz. The largest value obtained was 4.7 MHz. We conclude that the probability of the decorrelation bandwidth actually being close to 1 MHz is much less than 0.1%.

2.2.3. Fine-Scale Scintillation

A finer-scale variation within the scintillation maxima is apparent within the large-scale structures in Figure 1. This variation is not noise: it is a real modulation of intensity. Figure 3 shows an expanded view of part of a scintillation maximum in Figure 1. These finer-scale scintillations are also visible in the autocorrelation function, when the domain of integration is limited to a single peak of the scintillation spectrum in Figure 1. Analysis indicates that they have bandwidth $\Delta\nu \approx 0.5$ MHz and timescales of 1 to 3 minutes. The modulation index of this finer-scale structure is $m_f \approx 0.2$. These values are in approximate agreement with the scintillation parameters other groups have reported for PSR J0437–4715, as we discuss further in Paper 2.

3. Discussion

3.1. Scintillation Velocity

The combination of scintillation bandwidth and timescale yields an estimated velocity for the scintillation pattern, usually

dominated by the velocity of the pulsar. The relation (Gupta et al. 1994):

$$V_{ISS} = A_V \frac{\sqrt{\Delta\nu_{ISS} D x}}{v t_{ISS}} \quad (2)$$

connects scintillation velocity V_{ISS} to the observables $\Delta\nu_{ISS}$ and t_{ISS} , along with the distance of the pulsar D , an average fractional distance for the scattering material x , and a constant A_V . The calculated scintillation velocity V_{ISS} varies along with the scintillation bandwidth. Gothoskar et al. (2000) and Nicastro et al. (1995) both report variation of the inferred V_{ISS} by about a factor of 2, as inferred from individual observations. The V_{ISS} obtained for the wide-band scintillation, with $A_V = 3.85 \times 10^4 \text{ km s}^{-1} \times (1 \cdot \text{GHz} \cdot 1 \text{ sec})(1 \text{ MHz} \cdot 1 \text{ kpc})^{-1/2}$ (see Gupta et al. 1994), and an assumed distance of 150 pc (van Straten 2001), is 160 km s^{-1} . This is close to the average values of 170 km s^{-1} reported by Johnston et al. (1998), and not far from the 231 km s^{-1} reported by Gothoskar & Gupta (2000). The proper-motion velocity is 100 km s^{-1} (van Straten et al. 2001). Gothoskar & Gupta (2000) inferred from the relatively high scintillation velocity that the fractional distance of the scattering material, x (see Eq. 2), was larger than 1, and surmised that the scattering material likely lies at the surface of the Local Bubble. As discussed in Paper 2, evidence suggests that the scattering lies in a thin layer, ≈ 10 pc from the Sun.

3.2. Comparison with Other Pulsars

PSR J0437–4715 has among the lowest dispersion measures of strong pulsars, and it is perhaps unsurprising that the scintillation bandwidth is among the broadest observed, scaled to a single frequency. Comparisons with other pulsars are usually done by the typical pulse broadening time τ (actually the time required for a broadened pulse to reach $1/e$ of its maximum) (Pynzar’ & Shishov 1997). The scintillation bandwidth is related to the typical pulse broadening time, τ , by the equation:

$$\Delta\nu_{ISS} \tau = C_1 / (2\pi) \quad (3)$$

where C_1 is a constant of order unity (see Taylor et al. 1993, Lambert & Rickett 1999). We follow Pynzar’ & Shishov (1997) and adopt $C_1 = 1.0$, and scale to observing frequency $\nu = 300$ MHz using $\tau \propto \nu^{4.4}$. Figure 4 compares the scintillation parameters of PSR J0437–4715 with those of other pulsars. The broader- $\Delta\nu_{ISS}$ scattering of PSR J0437–4715 falls below the scaling found by Pynzar’ & Shishov (1997) for nearby pulsars, as does the scattering of PSR B0950+08 (Phillips & Clegg 1992).

Interestingly, the narrower- $\Delta\nu_{ISS}$ scattering of PSR J0437–4715 lies within the narrow region near the scaling expected for a homogeneous medium. So does some narrower-bandwidth structure reported in the dynamic spectrum of PSR B0950+08 (Roberts & Ables 1982). We will discuss a possible interpretation in a companion paper.

4. Conclusions

We find two scales of scattering for the nearby pulsar PSR J0437–4715. The broader scale has scintillation bandwidth

$\Delta\nu_{ISS} = 16_{-2}^{+5}$ MHz, and timescale $t_{ISS} = 1070 \pm 210$ sec. The narrower scale has $\Delta\nu_{ISS} = 0.5$ MHz, and timescale $t_{ISS} = 90$ sec. Both yield scintillation velocities close to the proper-motion velocity found by van Straten (2001). The pulse broadening time inferred from this scintillation bandwidth is less than that expected on the basis of observations of other nearby pulsars.

Acknowledgements. We thank the U.S. National Science Foundation for supporting this work.

References

- Cordes, J.M., & Lazio, T.J.W. 2002, astro-ph/0207156
 Desai, K. M., Gwinn, C. R., Reynolds, J. R., King, E. A., Jauncey, D., Flanagan, C., Nicolson, G., Preston, R. A., & Jones, D. L. 1992, ApJ, 393, L75
 Gothoskar, P., & Gupta, Y. 2000, ApJ, 531, 345
 Gupta, Y., Rickett, B. J., & Lyne, A. G. 1994, MNRAS, 269, 1035
 Gwinn, C. R., Britton, M. C., Reynolds, J. E. J., Jauncey, D. L., King, E. A., McCulloch, P. M., Lovell, J. E., & Preston, R. A. 1998, ApJ, 505, 928
 Hill, A.S., Stinebring, D.R., Barnor, H.A., Berwick, D.E., & Webber, A.B. 2003, ApJ, 599, 457
 Johnston, S., Nicastro, L., & Koribalski, B. 1998, MNRAS, 297, 108
 Lambert, H. C., & Rickett, B. J. 1999, ApJ, 517, 299
 Nicastro, L., & Johnston, S. 1995, MNRAS, 273, 122
 Phillips, J. A., & Clegg, A. W. 1992, Nature, 360, 137
 Pynzar', A.V., and Shishov, V.I. 1997, Astronomy Reports, 41, 586
 Roberts, J. A., & Ables, J. G. 1982, MNRAS, 201, 1119
 Smirnova T.V., Gwinn, C.R., & Shishov, V.I. 2005, submitted for publication (Paper 2).
 Stinebring, D. R., McLaughlin, M. A., Cordes, J. M., Becker, K. M., Espinoza Goodman, J. E., Kramer, M. A., Sheckard, J. L., & Smith, C. T. 2001, ApJ, 549, L97
 Taylor, J. H., Manchester, R. N., & Lyne, A. G. 1993, ApJS, 88, 529
 Thompson, A. R., Moran, J. M., & Swenson, G. W., Jr. 1986, Interferometry and Synthesis in Radio Astronomy, (New York: John Wiley & Sons)
 van Straten, W., Bailes, M., Britton, M., Kulkarni, S. R., Anderson, S. B., Manchester, R. N., & Sarkissian, J. 2001, Nature, 412, 158

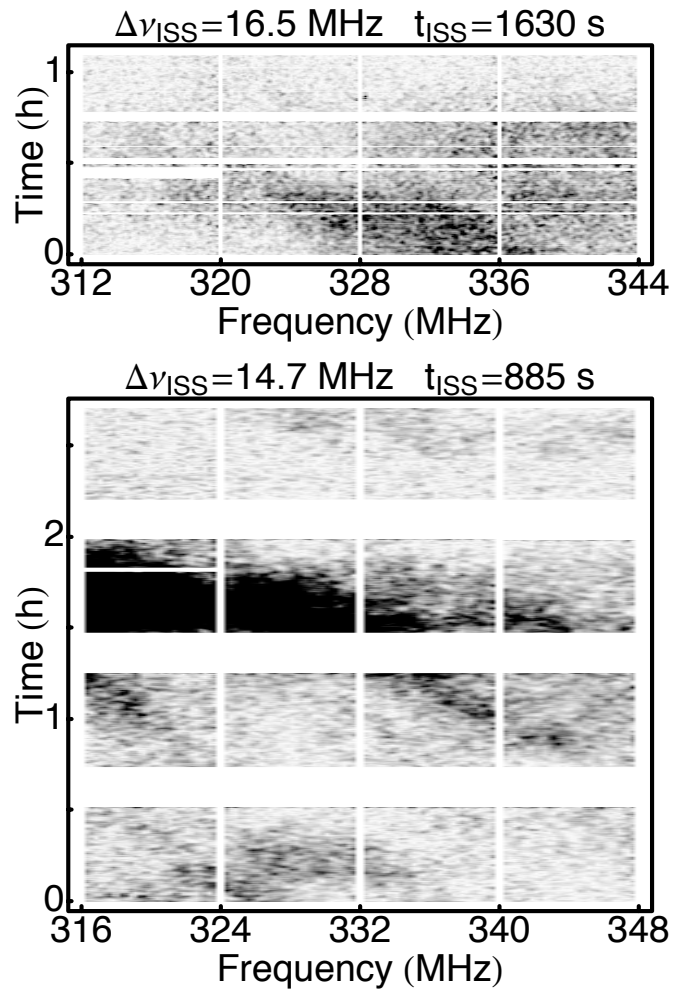


Fig. 1. Visibility amplitude as a function of frequency and time for observations of PSR J0437–4715 on the Fort Davis–Pie Town baseline on 5 November 1996 (bottom) and 8 April 1999 (top).

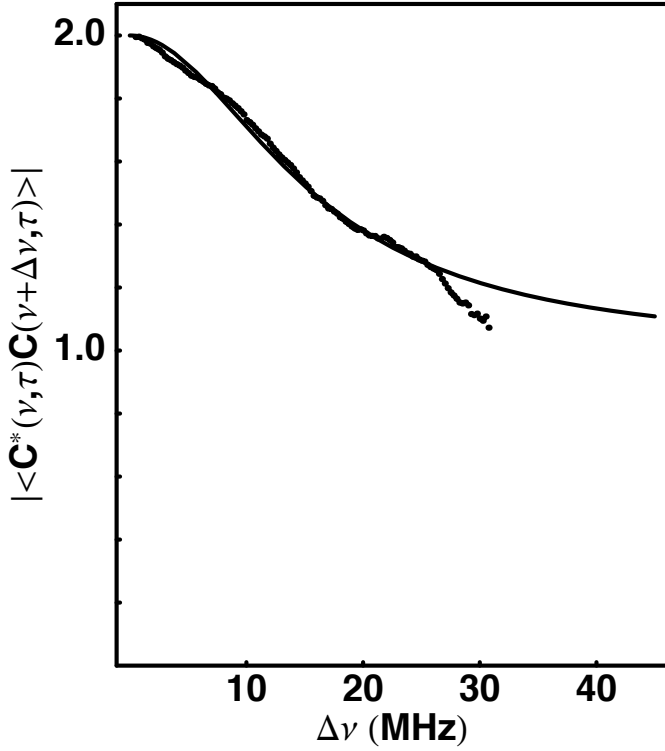


Fig. 2. The composite ACF obtained by suitably combining the ACFs from the two observations. The best-fitting Lorentzian has a characteristic width of $\Delta\nu_{ISS} = 15.7 \pm 0.2$ MHz.

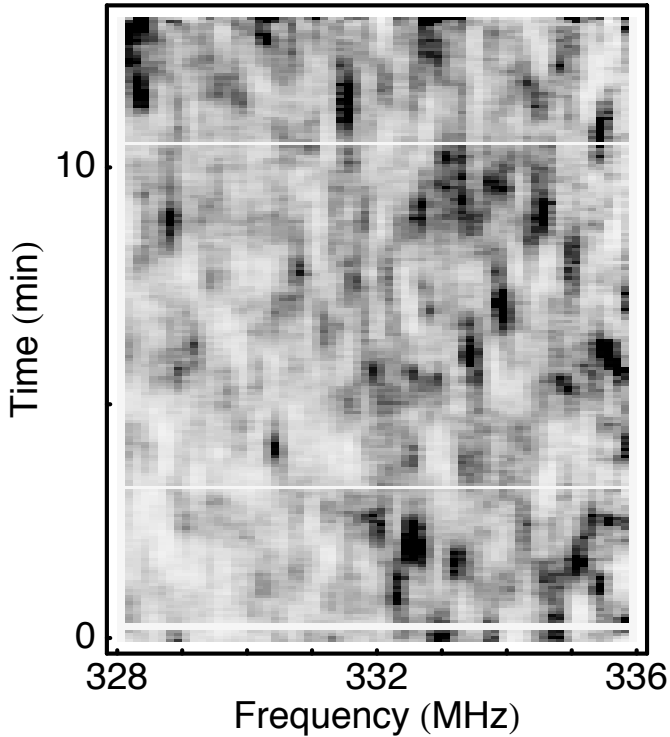


Fig. 3. Variations in the visibility amplitude within a scintillation maximum appear to occur over a frequency scale on the order of 1 MHz.

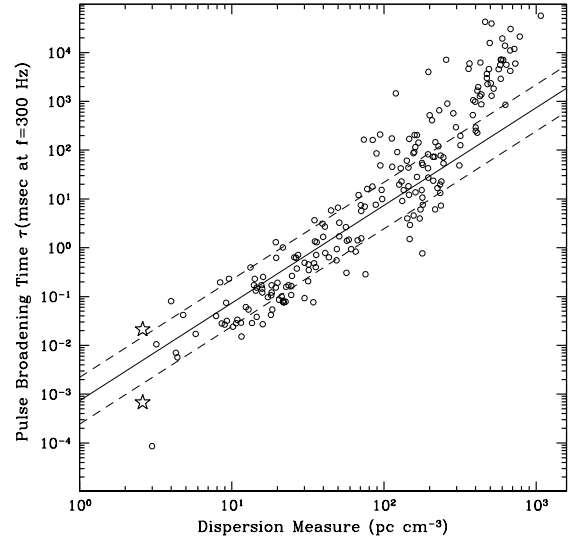


Fig. 4. Pulsar pulse broadening time plotted with dispersion measure, adapted from Pynzar' & Shishov (1997). As they discuss, the solid line shows the scaling of pulse broadening with distance expected for a uniform medium. Stars show the values we measured for PSR 0437–4715. Data for other pulsars from Cordes & Lazio (2002).

Table 1. Measured Scintillation Parameters for PSR J0437–4715

Epoch (MJD)	Wide-Bandwidth		Narrow-Bandwidth	
	$\Delta\nu_{ISS}$ (MHz)	t_{ISS} (sec)	$\Delta\nu_{ISS}$ (MHz)	t_{ISS} (sec)
50392	14.7	885	0.6	90
51276	16.5	1630	0.4	90
Composite	16_{-2}^{+5} ^a	1070 ± 210 ^a	0.5	90

^a Error estimated from Monte Carlo simulation.

List of Objects

‘PSR J0437–4715’ on page 1

‘PSR B0950+08’ on page 1